OXIDE INDUCED FATIGUE CRACK CLOSURE AND NEAR-THRESHOLD CHARACTERISTICS IN A508-3 STEEL

H. Kobayashi, T. Ogawa, H. Nakamura and H. Nakazawa

Department of Physical Engineering, Faculty of Engineering, Tokyo Institute of Technology, Tokyo, Japan

ABSTRACT

Crack closure in fatigue crack growth was measured successfully by two methods of ultrasonic and back face strain for an A508-3 steel. And the significance of crack closure to near-threshold characteristics in fatigue crack growth was clarified. Crack closure resulting from fretting oxide debris is of particular importance to near-threshold characteristics. The marked influence of stress ratio is due to oxide induced crack closure. When fretting oxide debris is excluded, plasticity induced crack closure becomes of importance to near-threshold characteristics and the marked influence of stress ratio disappears. A basic question on the measured crack closure levels still remains about the comparison of the two methods.

KEYWORDS

Fatigue; crack growth; threshold; crack closure; fretting oxide debris; stress ratio; ultrasonic; back face strain.

INTRODUCTION

In stage II, plane-strain, linear elastic fracture mechanics fatigue crack growth, growth rates, da/dN, under constant amplitude loading have been well related to stress intensity factor ranges, $\Delta K = K_{max} - K_{min}$, where K_{max} and K_{min} are maximum and minimum stress intensity factors, respectively. At intermediate ΔK values (stage IIb, striation mechanism), this relation takes a simple power law (Paris, 1963)

$$da/dN = C\ \Delta K^m \qquad (1)$$

where m and C are supposed to be material constants. A double-logarithmic plot of da/dN versus ΔK would then be a straight line, as shown in Fig. 1. Crack growth characteristics in stage IIb are insensitive to microstructure, environment and the stress ratio, $R = K_{min}/K_{max}$, and have been explained on the basis of plasticity induced crack closure (Elber, 1971; Kobayashi, 1981). At low ΔK values (stage IIa), however, da/dN deviates from Eq. (1) and

decreases abruptly to a vanishingly small value. Conceivably there is a threshold value of ΔK, namely ΔK_{th}, below which no crack growth occurs at all, as shown in Fig. 1. Near-threshold characteristics are very sensitive to microstructure, environment and R and have been explained on the basis of fretting oxide induced crack closure (Stewart, 1980; Suresh, 1981) or fracture surface roughness induced crack closure (Minakawa, 1981). Questions still remain, however, with respect to the specific influence of the above-mentioned factors.

The object of the present study is to develop an improved understanding of near-threshold characteristics through further consideration of crack closure and the influence of R.

MATERIAL AND EXPERIMENTAL PROCEDURE

The material used was an A508-3 steel (chemical composition, C/Si/Mn/P/S/Ni/Cr/Cu/Mo/V/Al: 0.18/0.22/1.46/0.0003/0.0005/0.69/0.15/0.05/0.57/<0.01/0.029

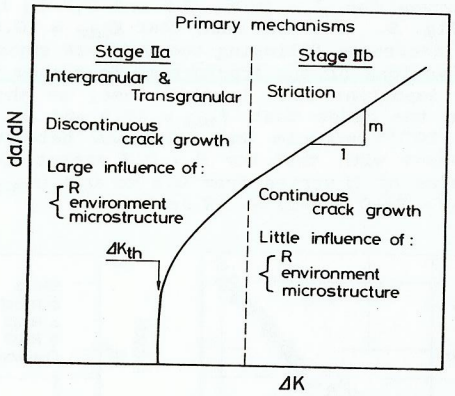

Fig. 1 Fatigue crack growth characteristics.

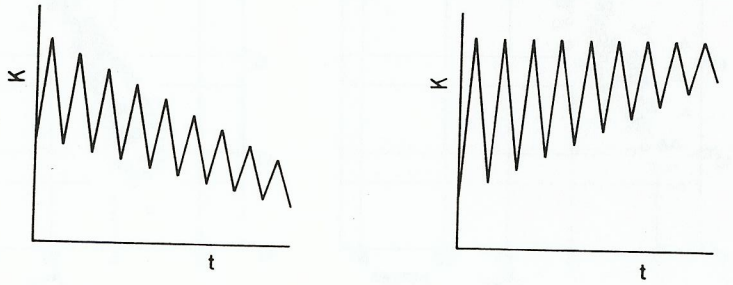

(a) R-constant test. (b) K_{max}-constant test.

Fig. 2 ΔK-decreasing test procedure.

wt. %; yield strength: 460 MPa; tensile strength: 595 MPa). Specimens used were of the ASTM compact type with W = 51.0 mm and B = 12.5 mm. The crack path was in the L-T orientation. The specimens were tested on a MTS feedback-controlled testing machine using load as the control parameter. Two types of tests, R-constant tests (R= 0.06, 0.3 and 0.7) and K_{max}-constant tests (K_{max} = 10.8, 15.5 and 31.0 MPa$\sqrt{m}$), were conducted in an air environment at room temperature. The test procedure was started by ΔK-decreasing conditions until ΔK_{th} was achieved. And then, the test was continued under ΔK-increasing conditions. The R-constant, ΔK-decreasing tests involve the stepping down of K_{max} and K_{min} for a given R value, as shown in Fig. 2 (a). On the other hand, the K_{max}-constant, ΔK-decreasing tests involve the stepping up of K_{min} for a given K_{max} value, as shown in Fig. 2 (b). Crack lengths were determined using a travelling microscope. In general, all of the testing and data analysis procedures for ASTM E647 (ASTM, 1981a) and an ASTM E24.04 working document (ASTM, 1981b) were adhered to. Crack closure was measured by two methods of ultrasonic (UT) and back face strain (BFS). In the UT-method, a 5 mm diameter, 10 MHz compession prove was used to monitor the specularly refrected signal, ΔE, from a growing fatigue crack during each load cycle. A typical P-ΔE curve is shown schematically in Fig. 3, where P, P_{max}, P_{min} and P_{op} are the cyclic, maximum, minimum and crack opening loads, respectively. In the BFS-method, a 2 mm strain gauge was mounted on the back face of the specimen to monitor the BFS, ε, during each load cycle. A typical P-ε curve is shown schematically in Fig. 4 (a). The linear portion of the P-ε curve was subtructed by using a differential electric curcuit, as shown schematically in Fig. 4 (b), where ε' is the subtracted BFS. In both methods, the values of P_{op} were determined as deviation points, c, from linear portions of the curves, c-d, during each load cycle, as shown in Figs. 3 and 4.

RESULTS

Figure 5 shows relations between da/dN and ΔK in the R-constant tests. For the cases that R = 0.06 and 0.3, da/dN deviates from Eq. (1) and decreases abruptly as ΔK decreases below 10 MPa$\sqrt{m}$. Fretting oxide debris exist on the fracture surface corresponding to these regions, as shown in Fig. 6, which may suggest that oxide induced crack closure has an important role on near-threshold characteristics for these cases. For the case that R = 0.7, Eq. (1) stands above $da/dN = 10^{-10}$ m/cycle and the fretting oxide debris do not exist on the fracture surface, except a narrow zone corresponding to ΔK_{th}.

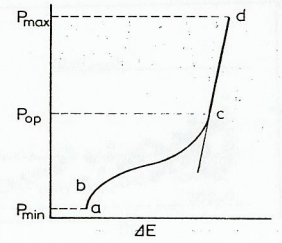

Fig. 3 Determination of P_{op} (UT-method).

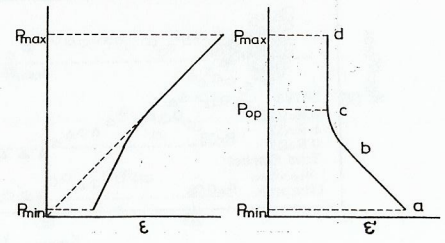

Fig. 4 Determination of P_{op} (BFS-method).

Figures 7 (a) and (b) show relations between K_{op}/K_{max} and K_{max} obtained by the UT- and BFS-methods, respectively, where K_{op} is an opening level of the stress intensity factor. When $K_{op} < K_{min}$, unloading was attempted to evaluate apparent K_{op} values which are denoted by solid symbols in Fig. 7. The values of K_{op}/K_{max} due to plasticity induced crack closure become nearly constant regardless of K_{max} for a given R value, except low K_{max} regions where K_{op}/K_{max} sweeps upward as K_{max} approaches threshold conditions due to oxide induced crack closure. There is a quantitive defference, however, between the K_{op}/K_{max} values measured by the two methods. So, a basic question on the measured crack closure levels still remains about the comparison of the two methods.

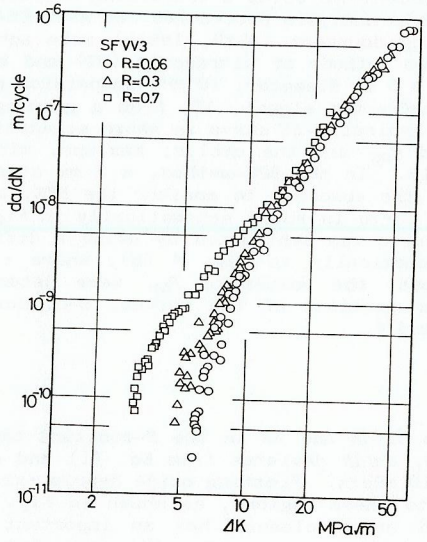

Fig. 5 Relations between da/dN and ΔK in R-constant tests.

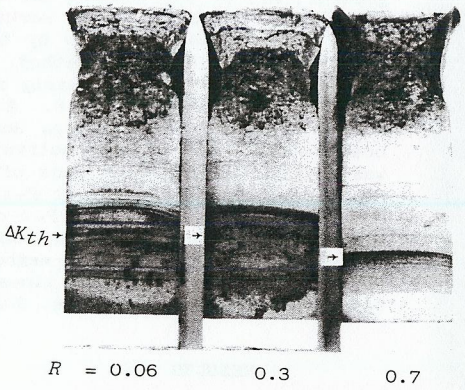

Fig. 6 Fracture surfaces in R-constant tests (fracture surfaces below and above arrows, ΔK_{th}, corespond to ΔK -decreasing and ΔK-increasing conditions, respectively).

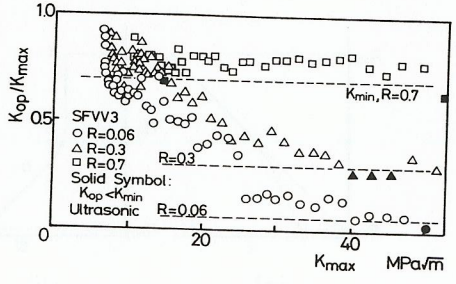

(a) UT-method

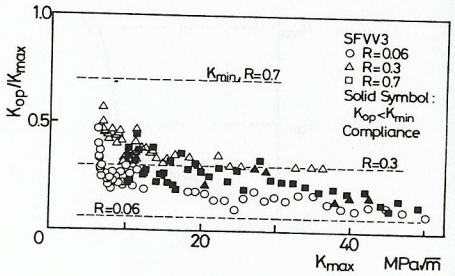

(b) BFS-method

Fig. 7 Relations between K_{op}/K_{max} and K_{max} in R-constant tests.

Figures 8 (a) and (b) show relations between da/dN and ΔK_{eff} obtained by the UT- and BFS-methods, respectively, where ΔK_{eff} is an effective stress intensity factor range ($\Delta K_{eff} = K_{max} - K_{op}$ for $K_{op} > K_{min}$ and $\Delta K_{eff} = K_{max} - K_{min}$ for $K_{op} < K_{min}$). The relations obtained by the UT-method become a following equation regardless of R

$$da/dN = C' \Delta K_{eff}^{m'} \qquad (2)$$

where C' is a material constant and $m' = 2$. On the other hand, Eq. (2) also stands for the results obtained by the BFS-method and $m' = 2.5$ regardless of R in the region that $da/dN \geq 5 \times 10^{-9}$ m/cycle, in which plasticity induced crack closure is dominant. In the region that $da/dN < 5 \times 10^{-9}$ m/cycle, however, da/dN deviates from Eq. (2) and decreases as ΔK_{eff} decreases especially for the cases that $R = 0.06$ and 0.3. For these cases, oxide induced crack closure is dominant, as shown in Fig. 6. So, it may be concluded that the BFS-method can not detect sufficiently oxide induced crack closure.

Figure 9 shows relations between da/dN and ΔK in the K_{max}-constant tests. The da/dN-ΔK curves for $R = 0.06$, 0.3 and 0.7 in the R-constant tests are also shown in Fig. 9. For the case that $K_{max} = 10.8$ MPa√m, da/dN decreases gradually as ΔK decreases following the da/dN-ΔK curves corresponding to each R value. Observations of the fracture surface show that oxide induced crack closure has an important role in this case, as shown in Fig. 10. On the other hand, for the cases that $K_{max} = 15.5$ and 31.0 MPa√m, Eq. (1) stands above $da/dN = 10^{-10}$ m/cycle and relations between da/dN and ΔK are in excellent agreement with that for $R = 0.7$ except ΔK_{th}, regardless of K_{max}, although the value of R varies from 0.3 to 0.8 ($K_{max} = 15.5$ MPa√m) or from 0.5 to 0.9 ($K_{max} = 31.0$ MPa√m) as ΔK decreases.

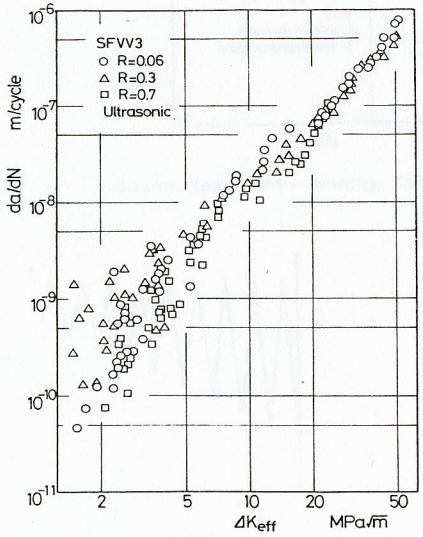

(a) UT-method

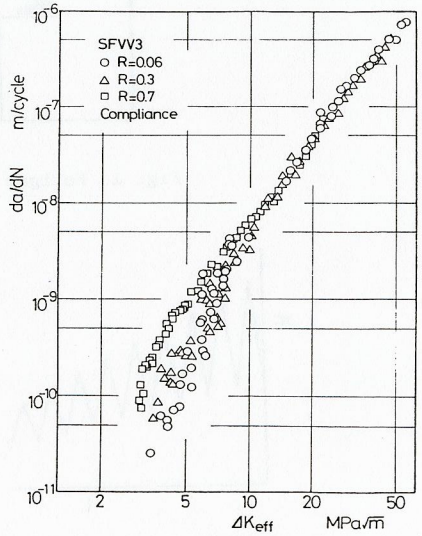

(b) BFS-method

Fig. 8 Relations between da/dN and ΔK_{eff} in R-constant tests.

The above-mentioned K_{max}-constant, ΔK-decreasing tests involve the stepping up of K_{min} and R for a given K_{max} value. In these cases, crack surfaces become difficult to contact, and then the fretting oxide debris can not accumulate behind the crack tip as ΔK decreases. This is a reason why the fretting oxide debris do not exist on the fracture surface at all.

That is to say, if a contribution of oxide induced crack closure is excluded, the near-threshold characteristics become insensitive to R and plasticity induced crack closure alone has an important role on them. The value of non-oxide controlled ΔK_{th}, determined at $da/dN = 10^{-10}$ m/cycle, becomes 2.7 MPa$\sqrt{m}$ regardless of R in this steel. It should be noted that a slightly higher value of ΔK_{th} for $R = 0.7$ is attributed to a little contribution of oxide induced crack closure as stated earlier.

After the R-constant, ΔK-decreasing tests, the specimens were sectioned and observations were carried out by a scanning electron microscope. A representative micrograph is shown in Fig. 11. The fretting oxide debris exist between the crack surfaces in the near-threshold region for a low R value. For a high R value, however, they do not exist, except a limited region corresponding to ΔK_{th}. As shown by Fig. 11, transgranular and intergranular shear modes of crack growth are dominant and the crack contour is rough, which may promote partial contact of crack surfaces (Minakawa, 1981). This is shown in Fig. 12 schematically. As a result, the fretting oxide debris are produced not uniformly but partially between the crack surfaces. That is to say, the fracture surface roughness may be a trigger for the production of the fretting oxide debris. So, both have a close relation each other.

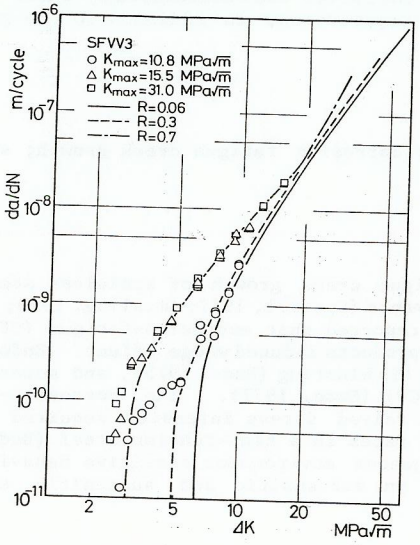

Fig. 9 Relations between da/dN and ΔK in K_{max}-constant tests.

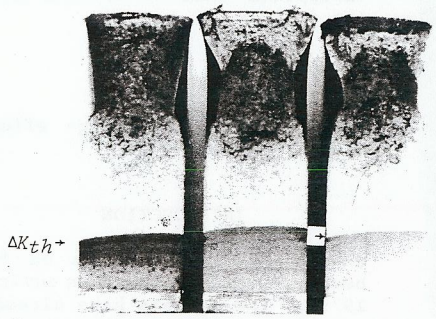

Fig. 10 Fracture surfaces in K_{max}-constant tests (fracture surfaces below arrows, ΔK_{th}, corespond to ΔK-decreasing conditions).

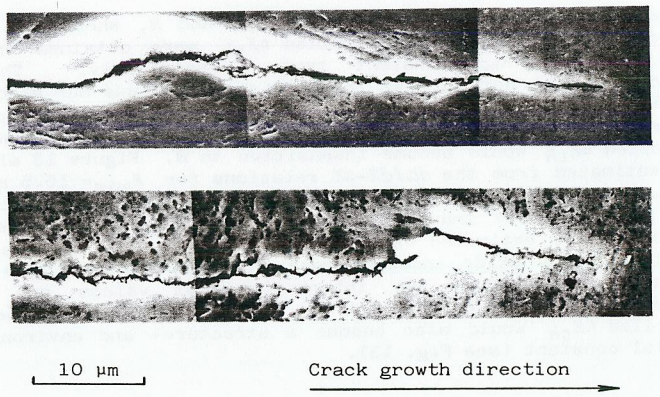

Fig. 11 Representative micrograph showing crack surface roughness and fretting oxide debris.

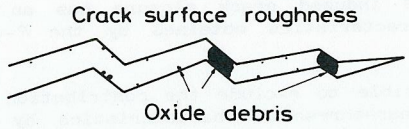

Fig. 12 Schematic diagram showing crack surface roughness and fretting oxide debris.

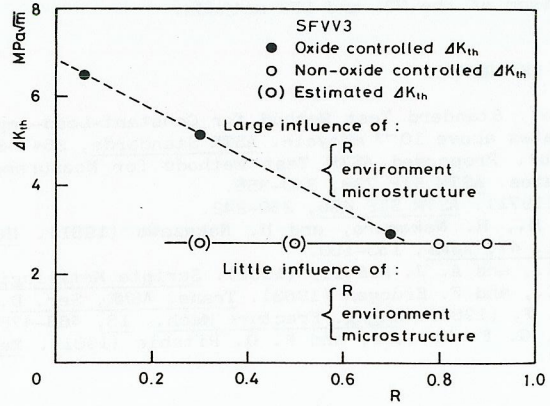

Fig. 13 Relations between ΔK_{th} and R in R- and K_{max}-constant tests.

DISCUSSIONS

Figure 13 shows relations between ΔK_{th} and R, where the values of oxide controlled and non-oxide controlled ΔK_{th} were obtained in the R-constant tests and the K_{max}-constant tests, respectively. The crack growth characterristics not only at intermediate ΔK values but also of near-threshold become insensitive to R, if the contribution of oxide induced crack closure is excluded (see Fig. 9). Likewise, the values of non-oxide controlled ΔK_{th} would become insensitive to R. Figure 13 also includes such data estimated from the da/dN-ΔK relations for K_{max}= 15.5 and 31.0 MPa$\sqrt{m}$ in the K_{max}-constant tests. In these cases, the characteristics are controlled only by plasticity induced crack closure. So, differences between oxide controlled and estimated ΔK_{th} for a given R value show quantitatively the contribution of oxide induced crack closure. In the case that the crack growth characteristics at intermediate ΔK values are insensitive to microstructure and environment as well as R, the values of non-oxide controlled ΔK_{th} would also become a structure- and environment-insensitive material constant (see Fig. 13).

CONCLUSIONS

The near-theshold characteristics in fatigue crack growth for the A508-3 steel were investigated. The results obtained are summarized as follows:

(1) Fretting oxide induced crack closure has an important role on the near-threshold characteristics obtained by the R-constant, ΔK-decreasing tests.

(2) It can be possible to exclude the contribution of oxide induced crack closure on the near-threshold characteristics by the K_{max}-constant, ΔK-decreasing tests. In this case, the characteristics are controlled only by plasticity induced crack closure.

(3) The values of non-oxide controlled ΔK_{th} become a material constant regardless of R in this steel.

(4) A basic question on the measured crack closure levels still remains about the comparison of the UT- and BFS-methods.

REFERENCES

ASTM (1981a). Standard Test Method for Constant-Load-Ampritude Fatigue Crack Growth Rates above 10^{-8} m/cycle. ASTM Standards, E647-81.

ASTM (1981b). Proporsed ASTM Test Methods for Measurement of Fatigue Crack Growth Rates. ASTM STP 738, 340-356.

Elber, W. (1971). ASTM STP 486, 230-242.

Kobayashi, H., H. Nakamura, and H. Nakazawa (1981). Mechanics of fatigue, AMD - Vol. 47, ASME, 133-150.

Minakawa, K., and A. J. McEvily (1981). Scripta Metallugica, 15, 633-636.

Paris, P. C., and F. Erdogan (1963). Trans. ASME, Ser. D, 85, 528-534.

Stewart, A. T. (1980). Engng. Fracture Mech., 13, 463-478.

Suresh, S., G. F. Zamiski, and R. O. Ritchie (1981). Metallug. Trans., 12A, 1435-1443.